A Naturally Heteroplasmic Clam Provides Clues about the Effects of Genetic Bottleneck on Paternal mtDNA

Mariangela Iannello[1,*], Stefano Bettinazzi[2], Sophie Breton[2], Fabrizio Ghiselli[1,*], and Liliana Milani[1]

[1]Department of Biological, Geological, and Environmental Sciences, University of Bologna, Italy

[2]Department of Biological Sciences, University of Montreal, Quebec, Canada

*Corresponding authors: E-mails: mariangela.iannello2@unibo.it; fabrizio.ghiselli@unibo.it.

Accepted: 3 February 2021

Abstract

Mitochondrial DNA (mtDNA) is present in multiple copies within an organism. Since these copies are not identical, a single individual carries a heterogeneous population of mtDNAs, a condition known as heteroplasmy. Several factors play a role in the dynamics of the within-organism mtDNA population: among them, genetic bottlenecks, selection, and strictly maternal inheritance are known to shape the levels of heteroplasmy across mtDNAs.

In Metazoa, the only evolutionarily stable exception to the strictly maternal inheritance of mitochondria is the doubly uniparental inheritance (DUI), reported in 100+ bivalve species. In DUI species, there are two highly divergent mtDNA lineages, one inherited through oocyte mitochondria (F-type) and the other through sperm mitochondria (M-type). Having both parents contributing to the mtDNA pool of the progeny makes DUI a unique system to study the dynamics of mtDNA populations. Since, in bivalves, the spermatozoon has few mitochondria (4–5), M-type mtDNA faces a tight bottleneck during embryo segregation, one of the narrowest mitochondrial bottlenecks investigated so far.

Here, we analyzed the F- and M-type mtDNA variability within individuals of the DUI species *Ruditapes philippinarum* and investigated for the first time the effects of such a narrow bottleneck affecting mtDNA populations. As a potential consequence of this narrow bottleneck, the M-type mtDNA shows a large variability in different tissues, a condition so pronounced that it leads to genotypes from different tissues of the same individual not to cluster together. We believe that such results may help understanding the effect of low population size on mtDNA bottleneck.

Key words: heteroplasmy, mitochondrial DNA, doubly uniparental inheritance, Bivalvia, high-throughput sequencing.

Significance

Several works aimed to investigate the role of different factors in affecting the within-individual mtDNA variability. Particularly, how different genetic bottleneck sizes during development may affect the distribution of mtDNA variants in the adult is often mathematically simulated. A unique model to study this topic is given by DUI species, in which mitochondria from males are transmitter to the next generation. Since the whole paternal mtDNA population comes from four to five sperm mitochondria, DUI species offer an unprecedented opportunity to investigate the effect of a small bottleneck on within-individual mitochondrial (mt) variability. Our results suggest that having such a narrow bottleneck profoundly impacts the segregation of mtDNA variants in different tissues, leading to possibly the highest within-individual mtDNA variability investigated so far.

Introduction

Mitochondria derive from ancient endosymbionts that are now firmly integrated into the biology of their host cell (Margulis 1970). Although most of the genes necessary for mt function have been horizontally transferred to the nucleus, mitochondria still maintain a genome, the mitochondrial DNA (mtDNA). In animals, it usually encodes for 37 genes, most of which are part of the translational machinery (22 transfer RNA

and two ribosomal RNA), whereas 13 code for proteins forming part of the respiratory complexes involved in the oxidative phosphorylation process (Boore 1999; Breton et al. 2014). Because the remaining mt proteins are translated from genes present in the nuclear (nu) genome, most respiratory complexes are in fact chimeric entities, in which both mt- and nu-encoded subunits must be compatible to preserve mt functions. Genomic incompatibilities can compromise the functioning of respiratory complexes, in turn potentially undermining fitness, fertility, and lifespan of individuals (Blier et al. 2001; Burton et al. 2006; Lane 2011; Latorre-Pellicer et al. 2016). As such, selection for intergenomic match likely represents a key force shaping the evolution of the joint mitonuclear genome, and, in turn, of eukaryotes (Lane 2011). Despite the need for mitonuclear compatibility, in animals, the mtDNA mutation rate is higher compared with the nu genome (i.e., 5–30 times) (Lane 2009; Payne et al. 2013; Wallace and Chalkia 2013). Evidence exists that the pace at which mtDNA mutates fosters compensatory mutations in the nu genome to maintain coadapted gene complexes, pointing to mtDNA variation as the main source of genetic variability fueling mitonuclear coevolution (Blier et al. 2001; Mishmar et al. 2006; Dowling et al. 2008).

In animals, the mt genome is usually strictly maternally inherited, and this situation was thought to be partly responsible for homoplasmy, a condition in which all mtDNAs are identical in an individual (Taylor and Turnbull 2005; Stewart and Chinnery 2015). Though homoplasmy would be ideal to prevent harmful genomic conflicts and promote optimal mt functions (Lane 2011), genetic variety in the mtDNA population is likely to be the common state in a cell (Taylor and Turnbull 2005; Payne et al. 2013; Aryaman, Bowles, et al. 2019; Klucnika and Ma 2019). The mtDNA is present in many copies within each cell and is constantly undergoing events of replication and degradation. Replication errors, together with potential oxidative damage (due to the proximity of the mt genome with the respiratory process), constitute the mechanisms by which mutations can rise and proliferate (Aryaman, Bowles, et al. 2019). This implies that each individual likely possesses a heterogeneous population of mtDNA variants, a condition termed heteroplasmy (Taylor and Turnbull 2005; Payne et al. 2013; Aryaman, Bowles, et al. 2019; Klucnika and Ma 2019). Modern sequencing techniques revealed that low levels of heteroplasmy are commonly present in many species of fungi, protists, plants, invertebrates, and vertebrates, including humans (Casane et al. 1994; Kann et al. 1998; Kmiec et al. 2006; Mjelle et al. 2008; He et al. 2010; Li et al. 2010; Magnacca and Brown 2010; Payne et al. 2013; Ye et al. 2014; Ding et al. 2015; Li et al. 2015; Naue et al. 2015; Robison et al. 2015; Meza-Lázaro et al. 2018; Klucnika and Ma 2019).

MtDNA populations are dynamic, and fluctuations in the proportion of mtDNA variants are common throughout the lifetime of individuals because of unequal partitioning of mtDNA molecules during cell division (vegetative segregation), random sampling of mtDNA molecules for replication (relaxed replication), and/or fission/fusion events among mitochondria (Stewart and Chinnery 2015; Aryaman, Johnston, et al. 2019; Ghiselli and Milani 2020; Heine and Hood 2020). In addition to neutral processes such as random genetic drift (Jenuth et al. 1996; Wonnapinij et al. 2008; Wilton et al. 2018), selection also plays a key role in shaping the landscape of mtDNA heterogeneity within organisms, tissues, cells, and even single mitochondria (Milani and Ghiselli 2015; Shtolz and Mishmar 2019). Haplotypes might be selected (positive selection) if beneficial for mt function or as a result of an intrinsic replicative advantage (Aryaman, Bowles, et al. 2019; Klucnika and Ma 2019). In animals, examples of the adaptive value of mtDNA stem from studies linking specific mtDNA variants with bioenergetic remodeling, increased longevity, adaptation to new environments or diets, and even speciation (Mishmar et al. 2003; Zhang et al. 2003; Ruiz-Pesini et al. 2004; Dowling et al. 2008; Gershoni et al. 2009; Lane 2009; Ji et al. 2012; Camus et al. 2017; Bettinazzi et al. 2019; Shtolz and Mishmar 2019). At the intra-individual level, positive selection could play a significant role in determining the distribution pattern of heteroplasmic mutations. In humans and mice, for example, accumulating evidence exists that the frequency of mtDNA variants differs substantially among tissues of the same individual, suggesting tissue-specific selective pressures for different heteroplasmic mutations (Jenuth et al. 1997; Chinnery et al. 1999; He et al. 2010; Samuels et al. 2013; Burgstaller et al. 2014; Li et al. 2015). Some tissues might be either more prone or susceptible to heteroplasmy because of difference in energetic needs. When considering the phenotypic effect of mtDNA variation, it is thus important to altogether account for the mutation itself, its abundance, and its segregation pattern in different tissues (Lane 2012; Shtolz and Mishmar 2019).

Even though evidence suggests that mtDNA variation can be adaptive, purifying (negative) selection is the main selective force driving the evolution of mtDNA through the removal of deleterious mutations (Ruiz-Pesini et al. 2004; Stewart et al. 2008; Li et al. 2010; Ye et al. 2014). mt heteroplasmy seems unfavorable for various biological systems (Lane 2012), and examples range from physiological, behavioral, and cognitive abnormalities in mice (Acton et al. 2007; Sharpley et al. 2012), to a wide range of clinic phenotypes in humans (Wallace and Chalkia 2013). To date, several hundred mtDNA mutations are associated with clinical disease (Taylor and Turnbull 2005; Wallace and Chalkia 2013; Stewart and Chinnery 2015). These mutant variants are usually heteroplasmic with the wild-type genome, and their proportion plays a critical role in determining a proper mt functioning within an individual. Uncompromised mt function can indeed be maintained until the abundance of mutant molecules exceeds a critical threshold level (usually around 70–90%), and the disease becomes evident (Taylor and Turnbull 2005; Wallace and Chalkia 2013; Stewart and Chinnery 2015). Given the high mtDNA mutation rate and the consequent accumulation of mtDNA genetic load, nu mechanisms apt to limit heteroplasmy and

intracellular competition likely take place (Havird et al. 2019). It is the case of the germline mt bottleneck during oocyte maturation that selectively eliminates the most severe mutations through a massive reduction of mtDNA molecules (Fan et al. 2008; Stewart et al. 2008; Samuels et al. 2010; Milani 2015; Milani and Ghiselli 2015; Zaidi et al. 2019). In addition, uniparental inheritance of cytoplasmic organelles has a central role in reducing the variability of the mtDNA population, virtually to a single haplogroup (Birky 1995; Christie et al. 2015).

In Metazoa, the only known exception to strictly maternal inheritance (SMI) is the doubly uniparental inheritance (DUI) of mitochondria, which is so far exclusively found in some bivalves (100+ species, see Gusman et al. 2016) and results in the inheritance of both maternal (F-type) and paternal (M-type) mtDNAs (Breton et al. 2007; Passamonti and Ghiselli 2009; Zouros 2013). In DUI bivalves, gametes only contain the sex-specific lineage (i.e., oocytes carry the F-type and spermatozoa the M-type lineage), whereas somatic tissues are mostly homoplasmic for the F-type in female individuals, whereas they are often heteroplasmic in males, where M-type is present in variable amounts (Ghiselli et al. 2011; Zouros 2013; Breton et al. 2017; Ghiselli et al. 2019). The two sex-linked haplogroups evolve at a different rate and are highly divergent, bearing 8–40% of nucleotide divergence (Breton et al. 2007; Passamonti and Ghiselli 2009; Zouros 2013). Consequently, unlike SMI, DUI species undergo a situation in which two sex-linked mtDNA haplogroups coexist in a population and must interact with a common nu background to maintain viable mt functions. Recent evidence revealed that both DUI mt-lineages are actively transcribed in somatic tissues (Milani, Ghiselli, Iannello, et al. 2014; Breton et al. 2017) and translated (Ghiselli et al. 2019), and an adaptive value of both independently segregated mt-variants has been proposed (Bettinazzi et al. 2019; 2020). As such, the DUI system represents a unique model to test how variation in sequence (heteroplasmy) can vary within and between distinct sex-linked haplotypes, tissues, and individuals, providing insight on how selection shapes the landscape of mtDNA heterogeneity and mt evolution (Milani and Ghiselli 2020).

In this study, we exploited the DUI system in the species *Ruditapes philippinarum* to investigate the within-individual variability of maternally and paternally inherited mt populations. In particular, we investigated for the first time the segregation of paternally inherited mtDNA in different tissues. Our results show that male individuals of *R. philippinarum* present a large variability in the M-type mtDNA populations from different tissues, providing new insights into the dynamics of mt genetic bottleneck and mt segregation.

Materials and Methods

mt Enrichment Protocol

Since there were no previously described mt enrichment protocols optimized specifically for *R. philippinarum*, we modified the protocol in Cherkasov et al. (2006). We sampled individuals of *R. philippinarum* from the Northern Adriatic Sea, in the river Po delta region (Sacca di Goro, approximate GPS coordinates: 44°50′06″N, 12°17′55″E) in June 2015. During this period, gametes are differentiating; therefore, for most samples, it was possible to determine the sex by microscope inspection of gonads. In these animals, gonads develop every year starting from germ line cells inside the visceral mass (in the connective tissue close to the intestine; Milani et al. 2017) and, during maturation, they occupy a consistent part of the body. For this experiment, we sampled in mature animals the part of the body that mostly consists of gonadal tissue, but we cannot exclude the presence, although in minority, of somatic tissues, such as connective tissue/intestine. Therefore, from now on, we refer to "body" as the part of the body mainly consisting in gonadal tissue. To optimize the mt enrichment method, we used the same tissues we used for later experiment. For this reason, we collected adductor muscles and bodies of both males and females. Each sample was split in two equal parts, one used as control, in which no mt enrichment was performed (nontreated samples), and the other one used to test the effectiveness of the mt enrichment (treated samples). Nontreated samples were minced and homogenized. In treated samples only, we performed the following mt enrichment protocol: samples were placed in 1.5 ml of ice-cold isolation buffer [IB (pH 7.5): 400 mmol/l sucrose (136.91 g/l), 100 mmol/l KCl (3.45 g/l), 50 mmol/l NaCl (2.92 g/l), 16 mmol/l EGTA (6.08 g/l), 30 mmol/l Hepes (7.14 g/l); Cherkasov et al. 2006] in a 2 ml tube, and minced with scissors. Then, 0.5 ml of IB was added to fill the tube. Samples were homogenized with three passes (200 rpm) of a Potter–Elvenhjem homogenizer using a loosely fitting Teflon pestle (keeping the glass tube on ice). Homogenates of the samples were centrifuged for 10 min at 2,500 × g at 2 °C and the supernatant collected and centrifuged again for 10 min at 3,500 × g at 2 °C. The supernatant was then collected carefully without touching the pellet, centrifuged at 11,000 × g at 2 °C for 12 min, and the pellets (enriched in mitochondria) were stored at −80 °C.

Protocol Validation

To validate the efficiency of the mt enrichment protocol, we compared treated and nontreated samples using confocal microscope observation and real-time qPCR. For microscope observation, we labeled mitochondria and nuclei, respectively, with MitoTracker Green FM (Molecular Probes, Eugene, Oregon, USA) and TO-PRO-3 (Molecular Probes, Life Technologies), with the following protocol.

In both treated and nontreated samples, Mitotracker Green and TO-PRO-3 were added to a final concentration of 400 nM and 0.5 μM, respectively. Samples were incubated with the dyes 30 min at 37 °C and then centrifuged at 13,000 × g for 1 min. After discarding the supernatant, the pellet was

washed twice in 500 µl PBS at room temperature. The pellet was spread on a slide and visualized at the confocal microscope.

The ratio of mitochondria versus nuclei in treated and nontreated samples was assessed using a confocal microscope Leica SP2.

We further confirmed protocol validation using real-time qPCR. Real-time qPCR data of mt and nu genes in nontreated samples of *R. philippinarum* were available in Milani, Ghiselli, Iannello, et al. (2014). Since they collected body samples in the same reproductive stage as ours, we compared RT-qPCR of those nontreated samples to RT-qPCR of our treated sample. We extracted DNA from males of treated samples using the MasterPure Complete DNA and RNA Purification Kit (Epicentre). DNA quantification was performed on a StepOnePlus real-time PCR system (Thermo Fisher Scientific Inc.), using SYBR Green I chemistry. We used the same primers in Milani, Ghiselli, Iannello, et al. (2014)—design specifically for *R. philippinarum*—to determine the threshold cycle (C_t) of the M-type mt gene cytochrome b (*cytb_M*) and the nu gene 18S ribosomal RNA (*18S*) after the mt enrichment protocol. C_ts of mt and nu genes in treated samples were compared with those of nontreated samples in Milani, Ghiselli, Iannello, et al. (2014).

Sample Collection, DNA Extraction, and Illumina Sequencing

Despite the peculiarity of mt inherence in DUI species, no previous works investigated the variability of F- and M-type mtDNA populations within individuals. In this work, we focused particularly on differences in mtDNA mutations between tissues that transmit mtDNA to the next generation (gonads) and tissues that do not transmit mtDNA (somatic tissues). In addition, since the M-type mitochondria of spermatozoa need to be functional in males, we tested if 1 h of sperm swim (the span time spermatozoa normally show an active swimming in experimental conditions) may induce new mutations in the M-type mtDNA.

Males and females of *R. philippinarum* used for Illumina sequencing were collected in the same location indicated above (Sacca di Goro, approximate GPS coordinates: 44°50′06″N, 12°17′55″E) during the reproductive season (precisely during July 2015). Gonad ripeness was confirmed by sacrificing few samples and inspecting the presence of eggs or sperm with an optical microscope.

To investigate the differences in mtDNA between body and sperm in males and to investigate the potential appearance of mutations in sperm after swimming, we induced spawning in males. Spawning was obtained by mild thermal shock, alternating cycles of cold and warm (22–29 °C, respectively) artificial seawater (reverse-osmosis water with aquariology sea salt added), every 30 min. Using this method, we were able to induce the spawning of four males (males 1–4). For each of these males, we collected the body, sperm, and sperm after 1 h of swimming (sperm1h).

To investigate differences between somatic tissues and gonads, we chose the adductor muscle as somatic tissue for the following reasons: 1) It is a well distinct and recognizable tissue in the clam body; and 2) it is physically distant from the gonad and we took advantage of such peculiarity to prevent gonad contaminations in the somatic samples. We therefore collected adductors and bodies from six further males (males 12, 13, 14, 17, 18, and 19) and adductors and bodies from six females (females 10, 11, 21, 22, 23, and 24) (see supplementary table 1, Supplementary Material online, for the sample list). We performed the mt enrichment protocol as described in the paragraph above. In sperm samples, the protocol did not perform as well as in other tissues. Checking the samples at the optical microscope during the centrifugation steps, we noticed that many spermatozoa in the supernatant (a fraction that should have been discarded) still had their mitochondria. After unsuccessfully trying to improve the separation of the midpiece mitochondria from the spermatozoa with sonication and enzymatic digestion, we decided to sequence both the fractions (from now on "pellet" and "supernatant") from the enrichment protocol in case the sequencing of the mtDNA in the expected mt-enriched fraction was poor. After the mt enrichment protocol, DNA extraction was performed using the MasterPure Complete DNA and RNA Purification Kit (Epicentre). The extracted DNA was then quantified with a NanoDrop ND-1000. DNA-seq libraries were generated following the protocols described in Dunham and Friesen (2013). Fragmentation and size selection were performed to obtain fragments of 300–800 bp of length. Single samples were barcoded and pooled. Pooled samples were sequenced over two lanes (two technical replicates) of an Illumina HiSeq 2500 machine, using 150-bp paired-end reads.

Quality Filter and De Novo Assembly of mt Genomes

A schematic workflow of the steps we followed after the Illumina sequencing is shown in supplementary table 3, Supplementary Material online. Before pooling together reads from the two sequencing lanes, we ensured the absence of batch effects. Briefly, after performing quality trimming, we mapped reads on the available F- and M-type mt genomes (GenBank accession numbers AB065375 and AB065374, respectively) to correlate the number of mt mapping reads in the two lanes. Furthermore, we performed an SNP calling to correlate F and M genotypes. Poor quality samples were removed from the analyses. For a detailed description of these steps, see Supplementary Material online.

The list of final samples is reported in supplementary table 4, Supplementary Material online. For each sample, we used reads mapping to the NCBI mt genomes to assembly *de novo* F-type and M-type mt references. For this purpose, we tried two different assemblers: IDBA (Peng et al. 2012) and

NOVOplasty (Dierckxsens et al. 2017) with default parameters. We decided to use assemblies from IDBA since it performed better (see Results for details). Among the newly assembled mt genomes from different samples, we chose as new references the longest F- and M-type from body samples. The two mt genomes were annotated by blasting (BLAST, Altschul et al. 1990) gene sequences from the NCBI reference and manually curating start and stop codons. tRNAs were annotated with Arwen (Laslett and Canbäck 2008).

SNP Calling

Reads from each sample were mapped against the de novo assembled F- and M-type mt reference genomes, using BWA-MEM (Li and Durbin 2009) with default parameters. Then, we used SAMtools (Li et al. 2009) to retrieve reads that mapped univocally, with minimum mapping quality 10, and in which left and right reads aligned concordantly. Samples with reads mapping on F-type mt genome were merged together to generate an F-type vcf file; similarly, samples with reads mapping on M-type were used to generate the M-type vcf files. Both vcf files were produced with freebayes v1.2.0 (https://github.com/freebayes/freebayes) with the following parameters: base quality 10, mapping quality 30, ploidy 1, and pooled-continuous. We used VCFtools (Danecek et al. 2011) to filter vcf files according to base quality, mapping quality, AF, and SNP depth (non-ref-af 0.15, min GQ 20, minQ 30–minDP 36). VCFtools was also used to obtain both information about sequencing depth, allele counts, AF, and also to generate vcf files with subsets of samples. In cases of low sequencing depth, it is impossible to discern real SNPs from sequencing errors; for this reason, we decided not to consider SNPs with sequencing depth below 36 and AF below 0.15, as suggested in Rensch et al. (2016) and Li et al. (2010). In addition, we also decided to exclude from the analyses samples with a median sequencing depth < 30 (a less strict value compared with the filer used for SNPs, considering it was applied to the median sequencing depth across all the positions). We used the vcf-subset script to obtain SNPs in samples belonging to the same tissue and the fill-an-ac script to re-calculate AF. We used Circos v 0.69-6 (Krzywinski et al. 2009) to visualize SNP positions on mt genomes. R (R Core Team 2013) was used to cluster together samples based on their genotype. More in detail, we used the cor() function to calculate correlation among samples with the "pairwise.complete.obs" method and the heatmap() function to visualize clustered samples. The correlation matrix was also transformed in distance matrix (dist() function in R) and plot as *x* and *y* coordinates using a multidimensional scaling analysis (cmdscale() function in R). Finally, the prediction of SNP effects on mt proteins was evaluated with SnpEff v2.1a (Cingolani et al. 2012).

Results

mt Enrichment and Sequencing

The results of mt enrichment protocol validation are showed in supplementary figures 1 and 2, Supplementary Material online. At confocal microscope inspection, the number of nuclei in enriched samples was remarkably lower or absent compared with nontreated samples (supplementary fig. 1, Supplementary Material online). In addition, an increase of the mt target and a decrease of the nu target were observed in treated versus nontreated samples using RT-qPCR (supplementary fig. 2, Supplementary Material online).

We applied the mt enrichment protocol to the samples before DNA extraction and Illumina library preparation. Supplementary material tables 1 and 2, Supplementary Material online, report the sample list and the DNA quantification before and after Illumina library preparation, respectively. The library preparation failed in the adductors of three females; therefore, we excluded those samples from the Illumina sequencing. The number of sequenced reads for each sample, in the two lanes, is reported in Supplementary Materials. On average, each sample has 3.7 millions of sequenced reads. For a detailed description of quality check results and investigation of batch effects, see Supplementary Materials.

De Novo Assembly and Annotation of F- and M-Type mtDNA References

The list of final samples—after the filtering and quality check steps of the workflow in supplementary material table 3, Supplementary Material online (see Materials and Methods)—is reported in supplementary material table 4, Supplementary Material online. We attempted to assemble the mt genomes of each sample using two different tools: IDBA and NOVOplasty. IBDA performed better with these samples, since it was able to assemble longer mt genomes, with lengths comparable to the NCBI references (that were obtained by Sanger sequencing through primer walking). For this reason, we decided to use IDBA to obtain *de novo* mt genomes from our samples (supplementary table 5, Supplementary Material online). In male bodies and in most male adductors, we were able to assemble both F- and M-type genomes. We assembled the F-type genomes from almost all of the female samples, but not the M-type genomes (i.e., no reads were found in females for the M-type genome). One exception was the adductor of Female 21 (sample 33), for which we were able to assemble also the M-type genome. In sperm and sperm1h, we could not assemble the F-type genome, since no F-type reads were detected (as expected in the DUI system). Across the assembled mt genomes, we found differences in length among samples. Although some samples had incomplete mt genomes, others had the complete set of RNAs and CDS, correctly assembled in a unique

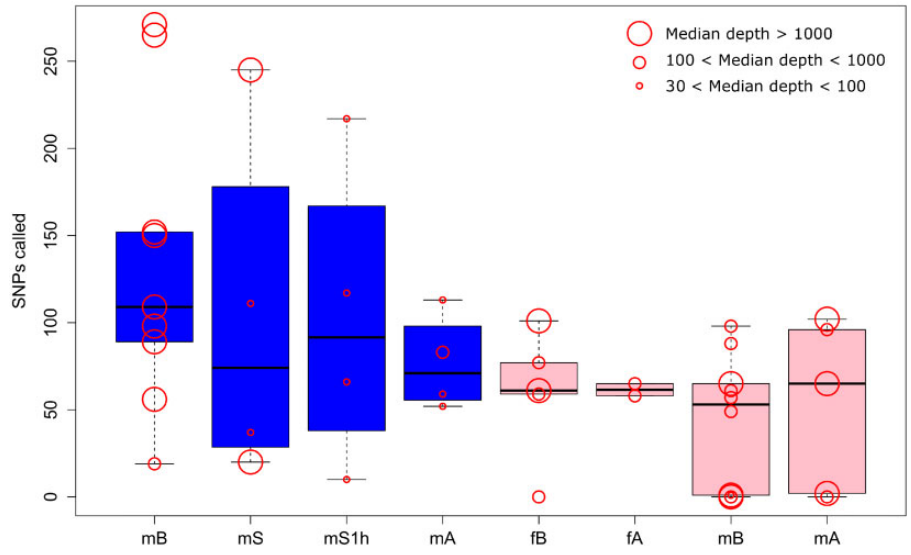

Fig. 1.—SNPs called in M- (dark blue) and F-type (pink) mt genome, separately for each condition. Circle dimension indicates median depth for each sample considered in this analysis. m, male samples; f, female samples; A, adductors; B, bodies; S, sperm; S1h, sperm after 1h swimming.

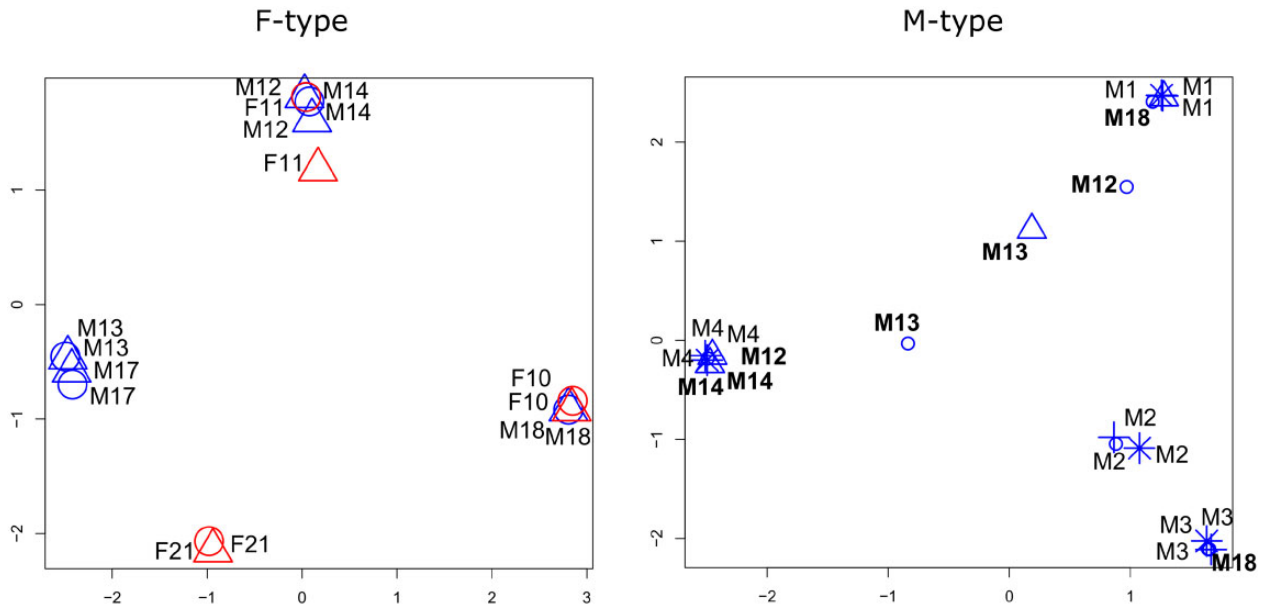

Fig. 2.—Samples clustered basing on their F- (left) and M-type (right) genotypes. Blue, males; red, females; O, body; Δ, adductor, +, sperm; *, sperm1h. Sample names in bold in M-type indicates within-sample comparisons between adductor and body; sample names not in bold indicates within-sample comparisons across body, sperm and sperm1h.

scaffold for each sample (scaffolds in bold in supplementary table 5, Supplementary Material online). These differences in length are probably due to variable repeats number in both F- and M-type mt genomes (length polymorphism due to variation in the number of repeated elements is common in bivalves; see Ghiselli et al. 2013; Guerra et al. 2014; Ghiselli et al. 2017) or not fully assembled control regions in some of these samples.

Assembly and Annotation of Reference Genomes

We chose, as new references, the longest *de novo* assembled F- and M-type mt genomes across male and female bodies (respectively, from the body of Male 19 and the body of Female 11). From the annotation of the new references, we found all the 13 protein-coding sequences and the two rRNAs in both F- and M-type mt genomes as well as 23 tRNAs in the

M-type genome and 24 tRNAs in the F-type (with an extra tRNA due to a duplication of the tRNA-M) (supplementary tables 6 and 7, Supplementary Material online). Furthermore, we solved some issues found in the annotation of the NCBI sequences, such as the misannotation of the *nad4L* gene in the F-type genome, the missing annotation of *atp8* genes in both F- and M-type, as well as the annotation of a new ORF with unknown function (ORFan), named *rphm21*, in the M-type genome (Ghiselli et al., 2013; Milani, Ghiselli, Maurizii, et al. 2014). The lists of annotated features, including coding sequences, tRNAs and rRNA, with the indication of start and stop codon, as well as the strand location, is reported in supplementary tables 6 and 7, Supplementary Material online.

F- and M-Type SNPs in Different Tissues

Reads from final samples (supplementary table 4, Supplementary Material online) were mapped against the new *de novo* assembled F- and M-type mt references. The number of mapping reads is reported in supplementary table 8, Supplementary Material online. The percentage of mapping reads varies considerably across samples ranging from 57% to less the 1%. The median sequencing depth per base of the two genomes in each sample is shown in supplementary table 9, Supplementary Material online. When the median sequencing depth of M- or F-type was below 30, we did not consider SNPs from that genome in that sample. Consequently, we removed F- and M-type genomes from S24 (M19 Adductor) and M-type genome from S22 (M17 adductor) from the analysis. Considering the sequencing depth, F-type genome is likely absent or extremely rare in sperm and sperm1h samples. On the other hand, male bodies and adductors present both genomes in different proportions. On average, in male bodies, the M-type genome sequencing depth is from three to nine times higher than F-type. On the contrary, in male adductors, F-type seems to be the prevalent genome, its sequencing depth being from 5 to 36 times higher than that of M-type. We did not find M-type reads in any of the females, with the exception of S33 (F21 adductor), in which F- and M-type are present at a 5:1 ratio.

Figure 1 shows the distribution of SNPs called in the two genomes for each tissue (see also supplementary tables 10 and 11, Supplementary Material online). The differences in the distributions are not statistically significant. The distribution of the minor allele frequency (MAF) in the F- and M-type, for each condition, is shown in supplementary figure 3, Supplementary Material online. The Kruskal–Wallis test confirmed the presence of significantly different distributions across conditions. We applied the Dunn test to perform multiple pairwise comparisons, with the Bonferroni correction. The *P* value for each comparison is reported in supplementary table 12, Supplementary Material online. MAF distributions in M-type male body, sperm, and sperm1h are significantly different from almost any other condition, whereas they are not different among each other. As shown in supplementary figure 3, Supplementary Material online, the MAF distributions are characterized by a predominant peak, corresponding to a frequency of 18%. All other conditions show a more uniform distribution of MAF, with the main peak at 25%.

Within-Individual mt Variability

To investigate the within-individual mt variability, we clustered samples according to their genotypes. Only individuals having more than one tissue successfully sequenced were used for this analysis. Correlation matrices for F- and M-type genotypes are reported in supplementary tables 13 and 14, Supplementary Material online. As shown in the multidimensional scaling analysis in figure 2, when we consider the F-type, tissues belonging to the same individual cluster together, both in females and in males. However, when we consider the M-type, the pattern looks different. Although body, sperm, and sperm1h belonging to the same individual always cluster together, adductor and body do not cluster together in three out of four individuals. A similar visualization, using heatmaps, is shown in supplementary figure 4, Supplementary Material online.

When investigating within-individual variants, we found a peculiar pattern of SNPs in shared positions within organisms. Considering the F-type and the M-type in male bodies and sperm, any time there is an SNP compared with the reference genome, tissues from the same individual share the same allele at that position (fig. 3, supplementary table 15, Supplementary Material online). But when we consider common M-type SNPs between male adductors and bodies, we found that in two out of four males (M12 and M18), most of the positions presents different alleles in the two tissues. In a third male (M13), the number of same alleles between adductor and body is comparable to that with different alleles, whereas in the last male (M14), the two tissues do not present different alleles at the same position (fig. 3, supplementary table 15, Supplementary Material online). A graphical representation of shared SNPs within the same individual is shown in figure 4. When we consider F-type (right side of the plot), most positions present the same allele within the same individual (green squares), both when we compare adductors and bodies in females and when we compare adductors and bodies in males. A similar situation can be observed when we compare shared mutations in the M-type of bodies and sperm (left side, blue shading). But when we consider shared SNPs positions between male adductors and bodies in the M-type, the proportion of different alleles (pink squares) is remarkable.

Figure 5 shows the comparison of allele frequency (AF) between tissues from the same individual. In most cases, we can see that the AF is comparable in all tissues considered within the same individual. This is the case in the comparison of AF between F-type SNPs in adductor and body both in females and

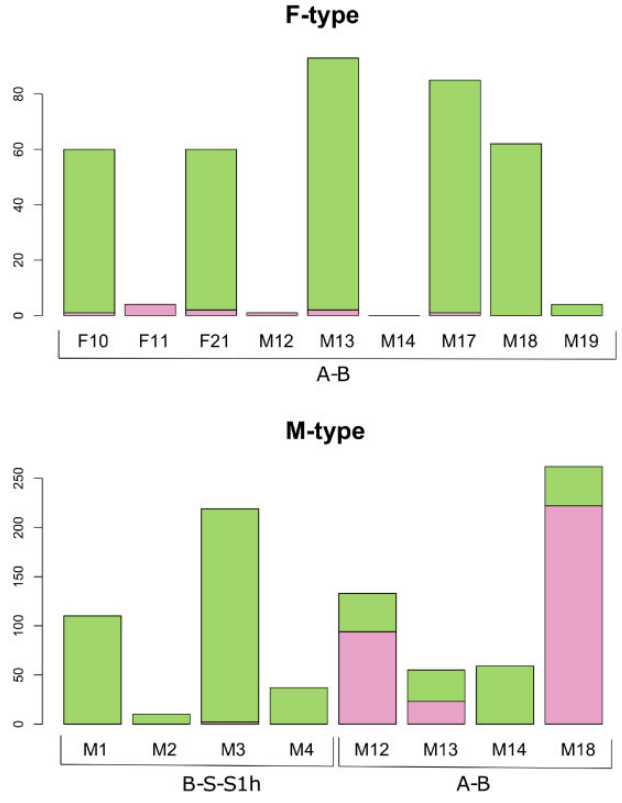

Fig. 3.—Number of F-type (top) and M-type (bottom) SNPs present in all tissues analyzed within the same individual. Green indicates the proportion of the same allele across tissues. Pink indicates the proportion of different alleles across tissues. For F11, only one tissue is reported (adductor) since the mtDNA in the body of F11 is the reference F-type genome used. m, male samples; f, female samples; A, adductors; B, bodies; S, sperm; S1h, sperm after 1h swimming.

males. In the same way, the AF is maintained when we compare body, sperm, and sperm1h from the same male individual. In all the above-mentioned within-individual comparisons, when an SNP is present in one tissue, its frequency is above 85% (considering that we cannot exclude the presence of low-frequency alleles), and this frequency is consistent across all the tissues from the same individual. However, this is not the case in the comparison between M-type SNPs in adductor and body from the same male individual. In particular, SNPs in the adductor may not be present in the body and vice versa (0% bars); furthermore, M-type in male adductor is the only condition where we find a consistent proportion of intermediate AF values, going from 0.2 to 0.8.

Evaluation of SNP Effects

SNPEff output gives a general idea of the effects of mutations on mt proteins (supplementary tables 16 and 17, Supplementary Material online). We found that the median percentage of synonymous SNP is higher in M-type genomes compared with F-type genomes. The percentage of SNP counts with a presumed silent effect (i.e., synonymous mutations) goes from 75 to 80 for M-type in male tissues, whereas it ranges from 59 to 62 for F-type in male and female tissues (supplementary fig. 5, Supplementary Material online); however, the differences across conditions are not statistically significant.

Discussion

Caveats and Limitations about the Investigated Organism

In this work, we exploited the DUI species *R. philippinarum* to investigate the fate of paternally inherited mtDNA in different male tissues. *R. philippinarum*, and bivalve molluscs in general, are far from being a model organism for genetics/genomics/evolutionary studies; as a consequence, most protocols and analyses must be revisited and optimized. For instance, no mt enrichment protocols were available for *R. philippinarum*. The aim of this step was to enrich the library in mt fraction and to reach an ultra-high sequencing depth that should have allowed the detection of very rare alleles in the mt populations. Nevertheless, we obtained quite different percentages of mtDNA reads in our samples, with sperm, for example, having a lower yield than other tissues. This difference in mapping reads across samples may be due to both biological and technical reasons. To ensure the robustness of our results, we decided to (1) keep only the positions with a good base and mapping quality and, concerning the within-sample comparison, to analyze just the positions having good quality in all of the tissues considered; (2) not consider minor allele frequencies below 15%.

To our knowledge, this is the first mtDNA high-throughput sequencing of F- and M-type mtDNAs from different tissues in a DUI species and, given the uniqueness of the biological system, also the first investigation performed on naturally heteroplasmic organisms with a remarkable mt-DNA sequence divergence.

Effect of Genetic Bottleneck on a Small mtDNA Population

The fate of a mtDNA population from oocyte to zygote to adult development is not straightforward and far from being fully understood. It is known to depend on several variables, most of them hard to evaluate. Both physical and genetic factors play a role in the dynamics of this peculiar within-organism population. Bottlenecks, different segregations in different cells, number of cell divisions, and within-mitochondria mtDNA copy number all contribute to generate variability between mothers and the offspring as well as across tissues and cells within the same individual. In addition, other factors deeply shape mtDNA populations such as genetic drift, selection, random or selective replication and degradation, recombination, mt fission/fusion, and transfer across cells (Johnston and Burgstaller 2019).

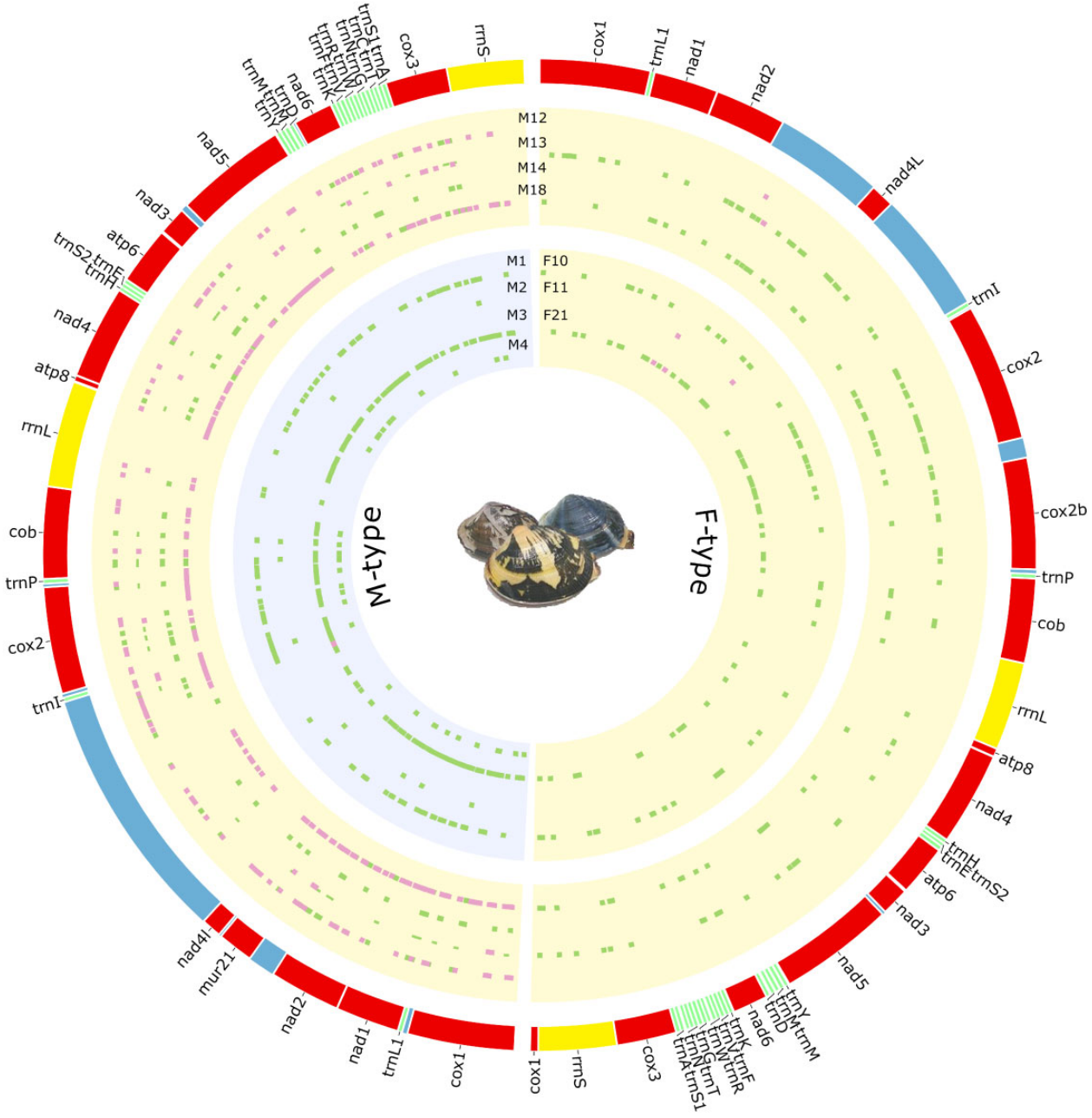

Fig. 4.—Graphical representation of shared SNPs within different tissues of the same individual. M-type SNPs are shown on the left side of the plot, F-type on the right side. SNPs sharing the same allele across tissues are represented in green, SNPs having different alleles are represented in pink. Yellow band, comparison between adductors and bodies; blue band, comparison between male gonad, sperm and sperm1h.

What makes this scenario even more intricate is the presence, in DUI species, of a second mtDNA population inherited through the sperm. This makes DUI a unique system to study the dynamics of mtDNA populations, especially to follow the destiny of the paternal mtDNA in natural conditions.

If, on one side, this system can help in understanding mt biology, dynamics, and interaction with the nucleus, on the other side, we have to face a series of complications, due to the fact that bivalves are evolutionarily distant from any model species. For instance, no indications about bottleneck sizes, number of replications during development, or even the embryonic origin of some tissues are available for bivalve species.

In this study, we analyzed the M- and F-type mtDNA variability within individuals of the DUI species *R. philippinarum*. What we observed is that the M-type mtDNA in male adductors is so different from that in male bodies (mature males that contain mainly gonadal tissue; see Materials and Methods section) that genotypes coming from the same individual do

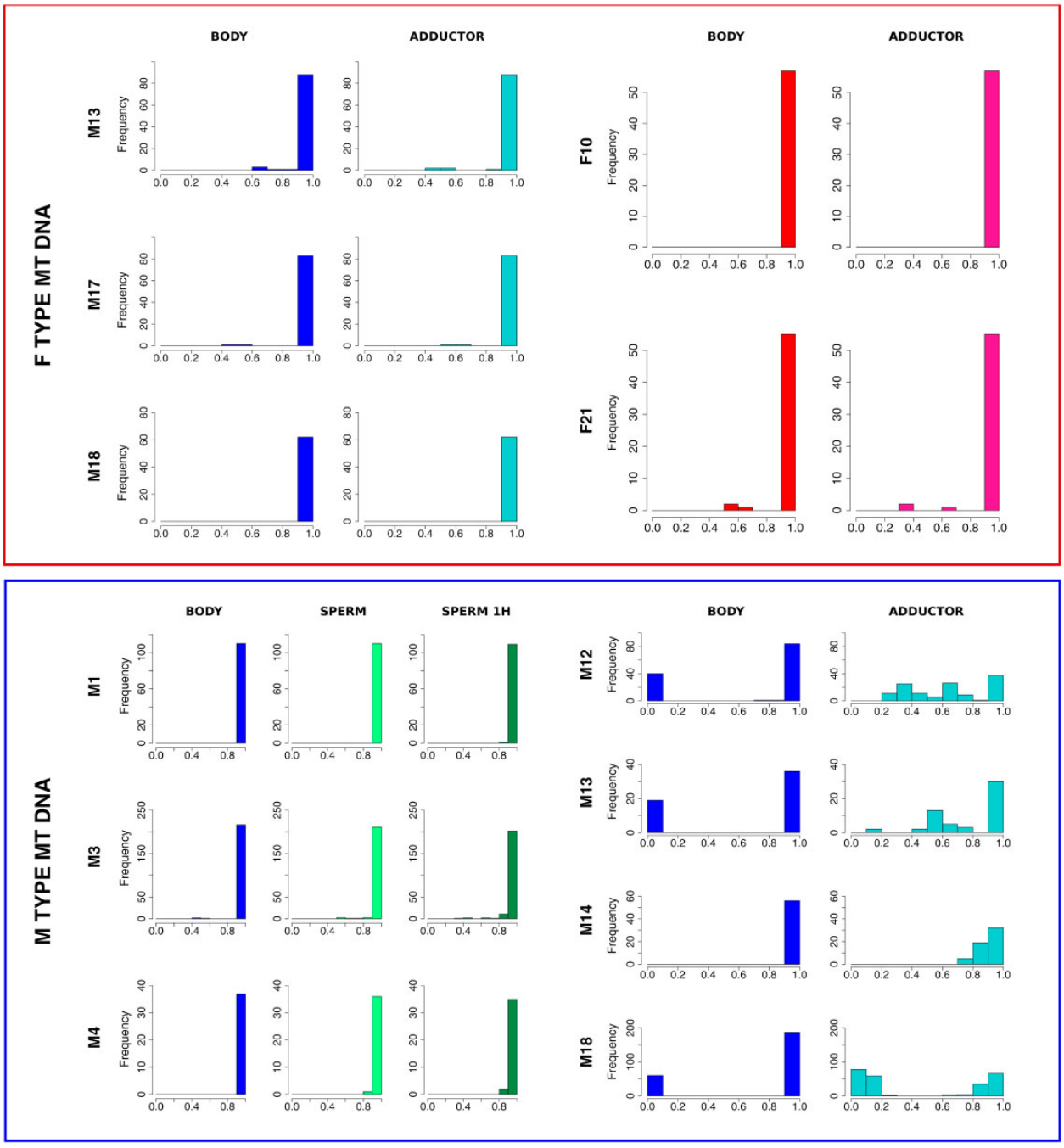

Fig. 5.—Allele frequency (AF) distribution of SNPs found in at least one tissue within the same individual. F-type AF are reported in the upper side of the figure (red square), M-type AF in the lower part of the plot (dark blue square). *x* axis = frequency of AF values and *y* axis = AF values.

not cluster together. On the other side, when we consider the F-type, samples cluster according to the individual both in males and in females. These differences in M-type mtDNAs are due to a peculiar pattern, found only in the adductor-body comparison: in three out of four males analyzed, when an SNP is found in one of the two tissues analyzed, in most cases, the other tissue is characterized by different alleles at that position. This condition is never observed when we compare male bodies and sperm, nor in the within-individual comparison of F-type SNPs in females or males. Such pattern, at a first sight, could be seen as a limited role of the M-type genome in male somatic tissues and a consequent relaxed selection on it. Nevertheless, it should be considered that 1) the percentage of nonsynonymous mutations (i.e., percentage of nonsynonymous mutations referred to the total number of mutations) affecting M-type genome is low (<25%) in all the male tissues

considered, with no statistically significant differences across conditions; and 2) there is no tissue-specific pattern of mutations (fig. 2); instead, M-type genotypes from male adductors cluster perfectly with male gonads from other individuals. Such results—that is, no tissue specific SNP clusters and higher percentage of synonymous mutations (compared with non-synonymous mutations) in all the male tissues considered—led us to exclude that the pattern of within-individual variability found in males was driven by a relaxed selection acting on male adductors.

Previous works in humans investigated the role of bottlenecks in changing AF distribution in different tissues (Rebolledo-Jaramillo et al. 2014; Li et al. 2015; Barrett et al. 2020). Here, we found that reference and alternative alleles are switched in most M-type SNPs of adductors and gonads. Even if we lack much information about developmental and mt biology of these animals, what we do know is that mtDNA from sperm faces an incredibly tight bottleneck. In fact, it is known that a spermatozoon of *R. philippinarum* carries four mitochondria (Milani et al. 2012), possibly with multiple copies of mtDNAs, but reasonably, a very low copy number, especially compared with the oocyte (Ghiselli et al. 2011).

It is well established that variance between the initial and final mutant proportion (for example between the zygote and a fully developed organism) in an mtDNA population depends on the mtDNA variability in the initial population and is inversely proportional to the genetic bottleneck (including both physical number of mtDNA and cell divisions). Therefore, cell-to-cell or tissue-to-tissue variability depends both on the initial mtDNA variability, sample size, and number of cell divisions. This means that, starting from the zygote, the higher number of mt genomes that segregate in different cells, the more similar the final population will be to the initial population (Johnston 2019). In the early embryo, possibly hundreds of thousands of mitochondria segregate in different cells during segmentation. During this period, mtDNA replication is stopped (Mishra and Chan 2014; Guerra et al. 2016). Only later during development, mtDNA begins to replicate. On the other side, only four paternal mitochondria are present in the zygote of *R. philippinarum*. Few studies have followed the fate of paternal mitochondria during the very first divisions of embryos in DUI species (Obata and Komaru 2005; Milani et al. 2011). According to Obata and Komaru (2005), if the embryo develops into a female, paternal mitochondria will disperse across cells and possibly will be degraded. On the contrary, if the embryo develops as a male, mitochondria aggregate during the first divisions and eventually end up in the 4d blastomere, probably, the precursor of the germline. This mechanism should ensure the presence of M-type mitochondria in male gonads and F-type in male somatic tissues. Anyway, different proportions of M-type mtDNA were detected in somatic tissues of DUI species (Ghiselli et al. 2011; Zouros 2013; Milani, Ghiselli, Iannello, et al. 2014), and M-type mt proteins were found in *R. philippinarum* early germ cells of both sexes (Ghiselli et al. 2019). In this work, we confirm that male adductors possess a variable amount of M-type mtDNA, even if in a lower amount compared with the F-type. This condition—that is, having heteroplasmic tissues for both the F- and M-type—was previously explained as a leakage of some mitochondria from the aggregate, a leakage that allows the segregation of mitochondria in other blastomeres and, eventually, in somatic tissues (Milani et al. 2012).

To the best of our knowledge, no maps of cell lineage fate regarding *R. philippinarum* development are available. The closest organisms where such studies have been conducted are gastropods (Hejnol et al. 2007; Lyons et al. 2012). Despite the disparity, it is believed that most spiralians share a conserved pattern in the development of homologous tissues (Lyons et al. 2012). Adductor muscles are known to develop from mantle in bivalves (Brusca et al. 2016). In gastropods, mantle can derive from several blastomeres, including 1a, 2a, 2b, 1c, 2c, and 2d but not 4d, which will give rise to the germline (fig. 6). If this is true also for bivalves, this means that mitochondria of the gonad and mitochondria of the adductor could split in the very first embryo division or at least within the first four divisions (fig. 6). Because of the extremely low number of initial M-type mitochondria (four) and the absence of mtDNA replication in this species until the veliger stadium (Guerra et al. 2016), one could suppose the whole mtDNA population of the adductor to derive from a single mitochondrion who escaped the mt aggregate. From this point on, the mtDNA populations of the somatic tissues and germ line will have totally different stories, and probably, they will be shaped by different physical and genetic dynamics. A very schematic representation of a possible scenario is represented in figure 6. Depending on how different was the mtDNA population in the "deserter" mitochondrion compared with the germ line mtDNA, different proportion of shared/different alleles will be observed. This would be in line with the results we obtained for the adductor-body comparisons in males. In fact, although, in two males (M12 and M18), the highest proportion of SNPs did not share the same allele in the two tissues, the same ratio of shared/different alleles was present in M13, and no differences at all were detected in M14. Our results are consistent with what predicted in Radzvilavicius et al. (2016) through simulations: according to that work, the high number of mitochondria in the egg suppresses mt variance across tissues during development, as drift is suppressed by large numbers. In our work, having the unique possibility to follow the segregation of the limited number of mitochondria from the sperm, we support such prediction. Indeed, as a potential consequence of such small number, a biased pattern of mt variants in different tissues is unequivocal.

Another interesting pattern is the tissue-specific difference in M-type AF distribution (fig. 5). Even if we cannot exclude the presence of low-frequency alternative alleles, we observed that all the variants investigated are fixed in the mtDNA

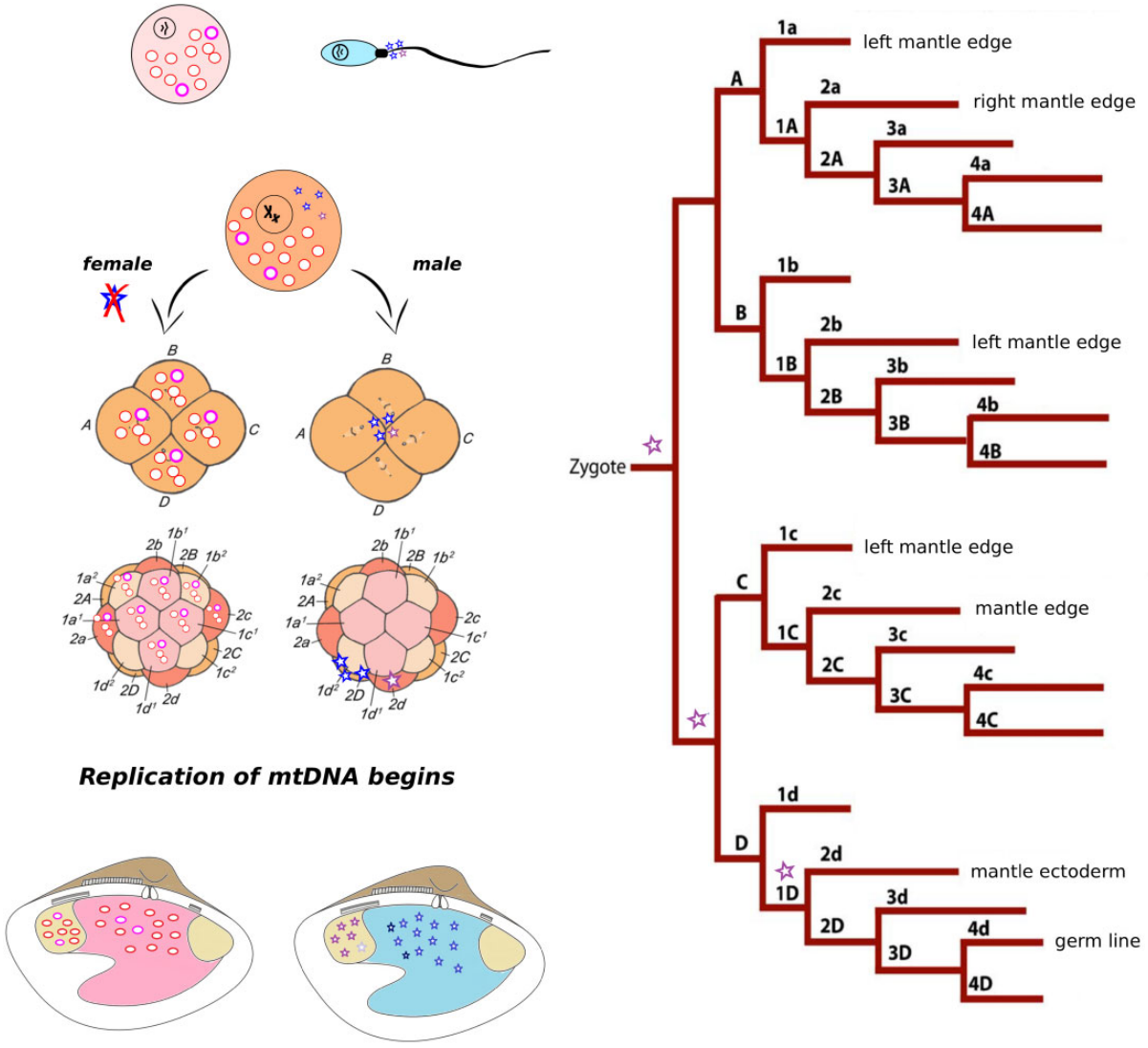

Fig. 6.—A simplified visualization of what may happen to maternal and paternal mtDNA population after mitochondria segregation during embryonic cell divisions. Stars and circles represent, respectively, M- and F-type mitochondria, and different colors indicate differences in mtDNA. For the sake of simplicity, only M-type mitochondria are shown in male embryo and tissues. Before fertilization, both sperm and egg carry their own mitochondrial population. The paternal mt population is much smaller compared to the maternal mt population. Depending on the dimension of this tiny paternal mt population, and on how different are the mtDNAs in paternal mitochondria, very different mt haplotypes may segregate in different cells during embryo development. Therefore, after cell proliferation, different tissues may be characterized by very different mtDNA populations within the same individual. On the other side, the maternal mtDNA population in the egg is much larger, therefore, the proportion of mt haplotypes that will segregate in different cells during embryo division will be more likely similar to what we find in the egg, and more similar across different tissues.The right side of the figure shows the cell lineage fate map of the gastropod *Crepidula fornicata*, since no fate map is available for *R. philippinarum*. If the fate of cells during the first divisions is conserved across these molluscs, the violet star indicates at which divisions the mitochondria from the adductor could segregate to the mitochondria that will populate the germ line.

population of male bodies and sperm samples. On the other hand, we see higher proportions of minor alleles in adductor samples. These differences in distributions may be due to both 1) stronger selection acting on male gonads and 2) more relaxed selection in adductors. According to (1), since M-type mtDNA in gonads and sperm will be transmitted to the next generation, it could be more subjected to selection compared with somatic tissues. How and when the selection shapes the mtDNA population would be something worthy to investigate in future analyses (see Milani and Ghiselli 2015). According to (2), the co-occurrence of F-type mitochondria in male adductors and, therefore, the co-occurrence of maternal mitochondria that can compensate for a potentially not optimal M-type mt activity could lead to a more relaxed selection acting on M-type mtDNA in such tissue ("selective arenas" hypothesis, see Stewart et al. 1996). However, when we investigated the effect of such mutations in adductor samples, we found that the percentage of silent mutations is comparable to that

found in male bodies and sperm and that it was higher than the percentage of silent mutations in F-type. Future analyses with a larger population size and multiple somatic tissues could help to clarify this point.

In conclusion, this work provides new insights into the genetic bottlenecks on mtDNA, giving for the first time the opportunity to investigate the effects of the smallest germline bottleneck analyzed so far in mtDNA populations. As a possible consequence of this narrow bottleneck, male individuals of *R. philippinarum* show large variability in the M-type mtDNA populations coming from different tissues. How does the nu DNA properly work together with both F- and M-type genomes and with so different M-type haplotypes is something that needs to be further investigated and that could help our understanding of mitonuclear interactions and mt dynamics.

Acknowledgments

This work was supported by the Italian Ministry of Education, University and Research (MIUR) SIR Programme grant No. RBSI14G0P5 funded to L.M., MIUR FIR2013 Programme grant No. RBFR13T97A funded to F.G., "Ricerca Fondamentale Orientata" (RFO) funding from the University of Bologna to L.M. and F.G., and the Canziani bequest funded to F.G.

Supplementary Material

Supplementary data are available at *Genome Biology and Evolution* online.

Data Availability

Raw reads from DNA sequencing are deposited on the SRA database (BioProject PRJNA639707); de novo F- and M-type reference genomes are available on GenBank (submission code: BankIt2356261); VCF files are available on figshare (https://figshare.com/s/274a1d3778093097a87a).

Literature Cited

Acton BM, Lai I, Shang X, Jurisicova A, Casper RF. 2007. Neutral mitochondrial heteroplasmy alters physiological function in mice. Biol Reprod. 77(3):569–576.

Altschul SF, Gish W, Miller W, Myers EW, Lipman DJ. 1990. Basic local alignment search tool. J Mol Biol. 215(3):403–410.

Aryaman J, Bowles C, Jones NS, Johnston IG. 2019. Mitochondrial network state scales mtDNA genetic dynamics. Genetics 212(4):1429–1443.

Aryaman J, Johnston IG, Jones NS. 2019. Mitochondrial heterogeneity. Front Genet. 9:718.

Barrett A, et al. 2020. Pronounced somatic bottleneck in mitochondrial DNA of human hair. Philos Trans R Soc B. 375(1790):20190175.

Bettinazzi S, Rodríguez E, Milani L, Blier PU, Breton S. 2019. Metabolic remodelling associated with mtDNA: insights into the adaptive value of doubly uniparental inheritance of mitochondria. Proc R Soc B. 286(1896):20182708.

Bettinazzi S, et al. 2020. Linking paternally inherited mtDNA variants and sperm performance. Philos Trans R Soc Lond B Biol Sci. 375(1790):20190177.

Birky CW. 1995. Uniparental inheritance of mitochondrial and chloroplast genes: mechanisms and evolution. Proc Natl Acad Sci USA. 92(25):11331–11338.

Blier PU, Dufresne F, Burton RS. 2001. Natural selection and the evolution of mtDNA-encoded peptides: evidence for intergenomic co-adaptation. Trends Genet. 17(7):400–406.

Boore JL. 1999. Animal mitochondrial genomes. Nucleic Acids Res. 27(8):1767–1780.

Breton S, Beaupré HD, Stewart DT, Hoeh WR, Blier PU. 2007. The unusual system of doubly uniparental inheritance of mtDNA: isn't one enough? Trends Genet. 23(9):465–474.

Breton S, et al. 2014. A resourceful genome: updating the functional repertoire and evolutionary role of animal mitochondrial DNAs. Trends Genet. 30(12):555–564.

Breton S, et al. 2017. The extremely divergent maternally- and paternally-transmitted mitochondrial genomes are co-expressed in somatic tissues of two freshwater mussel species with doubly uniparental inheritance of mtDNA. PLoS One 12(8):e0183529.

Brusca RC, Moore W, Shuster SM, Haver N. 2016. Invertebrates. Sunderland (MA): Sinauer Associates.

Burgstaller JP, et al. 2014. mtDNA segregation in heteroplasmic tissues is common in vivo and modulated by haplotype differences and developmental stage. Cell Rep. 7(6):2031–2041.

Burton RS, Ellison CK, Harrison JS. 2006. The sorry state of F2 hybrids: consequences of rapid mitochondrial DNA evolution in allopatric populations. Am Nat. 168(S6):S14–S24.

Casane D, Dennebouy N, de Rochambeau H, Mounolou JC, Monnerot M. 1994. Genetic analysis of systematic mitochondrial heteroplasmy in rabbits. Genetics 138(2):471–480.

Chinnery PF, et al. 1999. Nonrandom tissue distribution of mutant mtDNA. Am J Med Genet. 85(5):498–501.

Cingolani P, et al. 2012. A program for annotating and predicting the effects of single nucleotide polymorphisms. SnpEff Fly. 6(2):80–92.

Camus MF, Wolff JN, Sgrò CM, Dowling DK. 2017. Experimental support that natural selection has shaped the latitudinal distribution of mitochondrial haplotypes in Australian *Drosophila melanogaster*. Mol Biol Evol. 34(10):2600–2612.

Cherkasov AS, Ringwood AH, Sokolova IM. 2006. Combined effects of temperature acclimation and cadmium exposure on mitochondrial function in eastern oysters *Crassostrea virginica* gmelin (Bivalvia: Ostreidae). Environ Toxicol Chem. 25(9):2461.

Christie JR, Schaerf TM, Beekman M. 2015. Selection against heteroplasmy explains the evolution of uniparental inheritance of mitochondria. PLoS Genet. 11(4):e1005112.

Danecek P, et al. 2011. The variant call format and VCFtools. Bioinformatics 27(15):2156–2158.

Dierckxsens N, Mardulyn P, Smits G. 2017. NOVOPlasty: de novo assembly of organelle genomes from whole genome data. Nucleic Acids Res. 45(4):e18.

Ding J, et al. 2015. Assessing mitochondrial DNA variation and copy number in lymphocytes of ~2,000 sardinians using tailored sequencing analysis tools. PLoS Genet. 11(7):e1005306.

Dowling D, Friberg U, Lindell J. 2008. Evolutionary implications of non-neutral mitochondrial genetic variation. Trends Ecol Evol. 23(10):546–554.

Dunham JP, Friesen ML. 2013. A cost-effective method for high-throughput construction of illumina sequencing libraries. Cold Spring Harb Protoc. 2013(9):pdb.prot074187–834.

Fan W, et al. 2008. A mouse model of mitochondrial disease reveals germline selection against severe mtDNA mutations. Science 319(5865):958–962.

Gershoni M, Templeton AR, Mishmar D. 2009. Mitochondrial bioenergetics as a major motive force of speciation. BioEssays 31(6):642–650.
Ghiselli F, et al. 2013. Structure, transcription, and variability of metazoan mitochondrial genome: perspectives from an unusual mitochondrial inheritance system. Genome Biol Evol. 5(8):1535–1554.
Ghiselli F, et al. 2017. The complete mitochondrial genome of the grooved carpet shell, *Ruditapes decussatus* (Bivalvia, Veneridae). PeerJ. 5:e3692.
Ghiselli F, et al. 2019. Natural heteroplasmy and mitochondrial inheritance in bivalve molluscs. Integr Compar Biol. 59(4):1016–1032.
Ghiselli F, Milani L. 2020. Linking the mitochondrial genotype to phenotype: a complex endeavour. Philos Trans R Soc Lond B Biol Sci. 375(1790):20190169.
Ghiselli F, Milani L, Passamonti M. 2011. Strict sex-specific mtDNA segregation in the germ line of the DUI species *Venerupis philippinarum* (Bivalvia: Veneridae). Mol Biol Evol. 28(2):949–961.
Guerra D, Ghiselli F, Passamonti M. 2014. The largest unassigned regions of the male- and female-transmitted mitochondrial DNAs in *Musculista senhousia* (Bivalvia Mytilidae). Gene 536(2):316–325.
Guerra D, Ghiselli F, Milani L, Breton S, Passamonti M. 2016. Early replication dynamics of sex-linked mitochondrial DNAs in the doubly uniparental inheritance species *Ruditapes philippinarum* (Bivalvia Veneridae). Heredity 116(3):324–332.
Gusman A, Lecomte S, Stewart DT, Passamonti M, Breton S. 2016. Pursuing the quest for better understanding the taxonomic distribution of the system of doubly uniparental inheritance of mtDNA. PeerJ 4:e2760.
Havird JC, et al. 2019. Selfish mitonuclear conflict. Curr Biol. 29(11):R496–R511.
He Y, et al. 2010. Heteroplasmic mitochondrial DNA mutations in normal and tumour cells. Nature 464(7288):610–614.
Heine KB, Hood WR. 2020. Mitochondrial behaviour, morphology, and animal performance. Biol Rev. 95(3):730–737.
Hejnol A, Martindale MQ, Henry JQ. 2007. High-resolution fate map of the snail *Crepidula fornicata*: the origins of ciliary bands, nervous system, and muscular elements. Dev Biol. 305(1):63–76.
Jenuth JP, Peterson AC, Fu K, Shoubridge EA. 1996. Random genetic drift in the female germline explains the rapid segregation of mammalian mitochondrial DNA. Nat Genet. 14(2):146–151.
Jenuth JP, Peterson AC, Shoubridge EA. 1997. Tissue-specific selection for different mtDNA genotypes in heteroplasmic mice. Nat Genet. 16(1):93–95.
Ji F, et al. 2012. Mitochondrial DNA variant associated with Leber hereditary optic neuropathy and high-altitude Tibetans. Proc Natl Acad Sci USA. 109(19):7391–7396.
Johnston IG. 2019. Varied mechanisms and models for the varying mitochondrial bottleneck. Front Cell Dev Biol. 7:294.
Johnston IG, Burgstaller JP. 2019. Evolving mtDNA populations within cells. Biochem Soc Trans. 47(5):1367–1382.
Kann LM, Rosenblum EB, Rand DM. 1998. Aging, mating, and the evolution of mtDNA heteroplasmy in *Drosophila melanogaster*. Proc Natl Acad Sci. 95(5):2372–2377.
Klucnika A, Ma H. 2019. A battle for transmission: the cooperative and selfish animal mitochondrial genomes. Open Biol. 9(3):180267.
Kmiec B, Woloszynska M, Janska H. 2006. Heteroplasmy as a common state of mitochondrial genetic information in plants and animals. Curr Genet. 50(3):149–159.
Krzywinski M, et al. 2009. Circos: an information aesthetic for comparative genomics. Genome Res. 19(9):1639–1645.
Lane N. 2011. Mitonuclear match: optimizing fitness and fertility over generations drives ageing within generations. BioEssays. 33(11):860–869.
Lane N. 2012. The problem with mixing mitochondria. Cell. 151(2):246–248.
Laslett D, Canbäck B. 2008. ARWEN: a program to detect tRNA genes in metazoan mitochondrial nucleotide sequences. Bioinformatics. 24(2):172–175.
Latorre-Pellicer A, et al. 2016. Mitochondrial and nuclear DNA matching shapes metabolism and healthy ageing. Nature. 535(7613):561–565.
Li H, 1000 Genome Project Data Processing Subgroup, et al. 2009. The sequence alignment/map format and SAMtools. Bioinformatics. 25(16):2078–2079.
Li H, Durbin R. 2009. Fast and accurate short read alignment with Burrows-Wheeler transform. Bioinformatics. 25(14):1754–1760.
Li M, et al. 2010. Detecting heteroplasmy from high-throughput sequencing of complete human mitochondrial DNA genomes. Am J Hum Genet. 87(2):237–249.
Li M, Schröder R, Ni S, Madea B, Stoneking M. 2015. Extensive tissue-related and allele-related mtDNA heteroplasmy suggests positive selection for somatic mutations. Proc Natl Acad Sci USA. 112(8):2491–2496.
Lyons DC, Perry KJ, Lesoway MP, Henry JQ. 2012. Cleavage pattern and fate map of the mesentoblast, 4d, in the gastropod Crepidula: a hallmark of spiralian development. EvoDevo. 3(1):21.
Magnacca KN, Brown MJ. 2010. Mitochondrial heteroplasmy and DNA barcoding in Hawaiian Hylaeus (Nesoprosopis) bees (Hymenoptera: Colletidae). BMC Evol Biol. 10(1):174.
Margulis L. 1970. Origin of eukaryotic cells. New Haven (CT): Yale University Press.
Meza-Lázaro RN, Poteaux C, Bayona-Vásquez NJ, Branstetter MG, Zaldívar-Riverón A. 2018. Extensive mitochondrial heteroplasmy in the neotropical ants of the *Ectatomma ruidum* complex (Formicidae: Ectatomminae). Mitochond DNA Part A. 29(8):1203–1214.
Milani L. 2015. Mitochondrial membrane potential: a trait involved in organelle inheritance. Biol Lett. 11(10):20150732.
Milani L, Ghiselli F. 2015. Mitochondrial activity in gametes and transmission of viable mtDNA. Biol Direct. 10(1):22.
Milani L, et al. 2017. VASA expression suggests shared germ line dynamics in bivalve molluscs. Histochem Cell Biol. 148(2):157–171.
Milani L, Ghiselli F, Iannello M, Passamonti M. 2014. Evidence for somatic transcription of male-transmitted mitochondrial genome in the DUI species *Ruditapes philippinarum* (Bivalvia: Veneridae). Curr Genet. 60(3):163–173.
Milani L, Ghiselli F, Maurizii MG, Nuzhdin SV, Passamonti M. 2014. Paternally transmitted mitochondria express a new gene of potential viral origin. Genome Biol. Evol. 6(2):391–405.
Milani L, Ghiselli F, Maurizii MG, Passamonti M. 2011. Doubly uniparental inheritance of mitochondria as a model system for studying germ line formation. PloS One. 6(11):e28194.
Milani L, Ghiselli F, Passamonti M. 2012. Sex-linked mitochondrial behavior during early embryo development in *Ruditapes philippinarum* (Bivalvia Veneridae) a species with the doubly uniparental inheritance (DUI) of mitochondria. J Exp Zool. 318(3):182–189.
Milani L, Ghiselli F. 2020. Faraway, so close. The comparative method and the potential of non-model animals in mitochondrial research. Philos Trans R Soc Lond B Biol Sci. 375(1790):20190186.
Mishmar D, et al. 2003. Natural selection shaped regional mtDNA variation in humans. Proc Natl Acad Sci. 100(1):171–176.
Mishmar D, et al. 2006. Adaptive selection of mitochondrial complex I subunits during primate radiation. Gene. 378:11–18.
Mishra P, Chan DC. 2014. Mitochondrial dynamics and inheritance during cell division, development and disease. Nat Rev Mol Cell Biol. 15(10):634–646.
Mjelle KA, Karlsen BO, Jørgensen TE, Moum T, Johansen SD. 2008. Halibut mitochondrial genomes contain extensive heteroplasmic tandem repeat arrays involved in DNA recombination. BMC Genom. 9(1):10.

Naue J, et al. 2015. Evidence for frequent and tissue-specific sequence heteroplasmy in human mitochondrial DNA. Mitochondrion. 20:82–94.
Obata M, Komaru A. 2005. Specific location of sperm mitochondria in mussel *Mytilus galloprovincialis* zygotes stained by MitoTracker. Dev Growth Differ. 47(4):255–263.
Payne BAI, et al. 2013. Universal heteroplasmy of human mitochondrial DNA. Hum Mol Genet. 22(2):384–390.
Passamonti M, Ghiselli F. 2009. Doubly uniparental inheritance: two mitochondrial genomes, one precious model for organelle DNA inheritance and evolution. DNA Cell Biol. 28(2):79–89.
Peng Y, Leung HCM, Yiu SM, Chin FYL. 2012. IDBA-UD: a de novo assembler for single-cell and metagenomic sequencing data with highly uneven depth. Bioinformatics. 28(11):1420–1428.
R Core Team. 2013. R: a language and environment for statistical computing. Vienna (Austria): R Foundation for Statistical Computing. Available from: http://www.R-project.org/.
Radzvilavicius AL, Hadjivasiliou Z, Pomiankowski A, Lane N. 2016. Selection for mitochondrial quality drives evolution of the germline. PLoS Biol. 14(12):e2000410.
Rebolledo-Jaramillo B, et al. 2014. Maternal age effect and severe germline bottleneck in the inheritance of human mitochondrial DNA. Proc Natl Acad Sci USA. 111(43):15474–15479.
Rensch T, Villar D, Horvath J, Odom DT, Flicek P. 2016. Mitochondrial heteroplasmy in vertebrates using ChIP-sequencing data. Genome Biol. 17(1):139.
Robison GA, Balvin O, Schal C, Vargo EL, Booth W. 2015. Extensive mitochondrial heteroplasmy in natural populations of a resurging human pest, the bed bug (Hemiptera: Cimicidae). J Med Entomol. 52(4):734–738.
Ruiz-Pesini E, Mishmar D, Brandon M, Procaccio V, Wallace DC. 2004. Effects of purifying and adaptive selection on regional variation in human mtDNA. Science 303(5655):223–226.
Samuels DC, Wonnapinij P, Cree LM, Chinnery PF. 2010. Reassessing evidence for a postnatal mitochondrial genetic bottleneck. Nat Genet. 42(6):471–472.
Samuels DC, et al. 2013. Recurrent tissue-specific mtDNA mutations are common in humans. PLoS Genet. 9(11):e1003929.
Sharpley MS, et al. 2012. Heteroplasmy of mouse mtDNA is genetically unstable and results in altered behavior and cognition. Cell 151(2):333–343.
Shtolz N, Mishmar D. 2019. The mitochondrial genome – on selective constraints and signatures at the organism, cell, and single mitochondrion levels. Front Ecol Evol. 7:342.
Stewart JB, et al. 2008. Strong purifying selection in transmission of mammalian mitochondrial DNA. PLoS Biol. 6(1):e10.
Stewart DT, Kenchington ER, Singh RK, Zouros E. 1996. Degree of selective constraint as an explanation of the different rates of evolution of gender-specific mitochondrial DNA lineages in the mussel Mytilus. Genetics 143(3):1349–1357.
Stewart JB, Chinnery PF. 2015. The dynamics of mitochondrial DNA heteroplasmy: implications for human health and disease. Nat Rev Genet. 16(9):530–542.
Taylor RW, Turnbull DM. 2005. Mitochondrial DNA mutations in human disease. Nat Rev Genet. 6(5):389–402.
Wallace DC, Chalkia D. 2013. Mitochondrial DNA genetics and the heteroplasmy conundrum in evolution and disease. Cold Spring Harbor Perspect Biol. 5(11):a021220–a021220.
Wilton PR, Zaidi A, Makova K, Nielsen R. 2018. A population phylogenetic view of mitochondrial heteroplasmy. Genetics 208(3):1261–1274.
Wonnapinij P, Chinnery PF, Samuels DC. 2008. The distribution of mitochondrial DNA heteroplasmy due to random genetic drift. Am J Hum Genet. 83(5):582–593.
Ye K, Lu J, Ma F, Keinan A, Gu Z. 2014. Extensive pathogenicity of mitochondrial heteroplasmy in healthy human individuals. Proc Natl Acad Sci USA. 111(29):10654–10659.
Zaidi AA, et al. 2019. Bottleneck and selection in the germline and maternal age influence transmission of mitochondrial DNA in human pedigrees. Proc Natl Acad Sci USA. 116(50):25172–25178.
Zhang J, et al. 2003. Strikingly higher frequency in centenarians and twins of mtDNA mutation causing remodeling of replication origin in leukocytes. Proc Natl Acad Sci USA. 100(3):1116–1121.
Zouros E. 2013. Biparental inheritance through uniparental transmission: the Doubly Uniparental Inheritance (DUI) of mitochondrial DNA. Evol Biol. 40(1):1–31.

Associate editor: Alexander Suh